Journal of the Geological Society, London, Vol. **171**, 2014, pp. 375–387. http://dx.doi.org/10.1144/jgs2013-086
Published *Online First* on March 20, 2014

Stratigraphic correlation of Holocene phonolitic explosive episodes of the Teide–Pico Viejo Volcanic Complex, Tenerife

OLAYA GARCÍA[1*], SILVINA GUZMÁN[2] & JOAN MARTÍ[1]
[1]*Instituto de Ciencias de la Tierra Jaume Almera, CSIC, Lluis Solé Sabarís s/n, 08028 Barcelona, Spain*
[2]*IBIGEO (CONICET-UNSa), Museo de Ciencias Naturales, Universidad Nacional de Salta, Mendoza 2, 4400, Salta, Argentina*
**Corresponding author (e-mail: garciaperez.olaya@gmail.com)*

Abstract: Teide and Pico Viejo (TPV) are twin stratovolcanoes that form one of the largest alkaline volcanic complexes in the world. They began forming inside the caldera of Las Cañadas about 200 ka ago and are largely made up of an accumulation of mafic, intermediate and more recent felsic products that form lava flows. However, a significant number of Holocene pyroclastic deposits are also present. To quantify the explosive contribution to the construction of TPV, we re-examined its stratigraphy and identified several Holocene phonolitic explosive episodes ranging from Strombolian to sub-Plinian styles that are represented by fallout and pyroclastic density current deposits. Although some of the pumice deposits have been related to known sources, a few have not been linked to a specific vent. The use of field data as well as geochemical and mineralogical analysis helped to provide reliable criteria for robust correlations and to establish the relative stratigraphy of the deposits. The presence of these pyroclastic deposits in the recent history of the TPV complex suggests that these stratovolcanoes are entering a more explosive stage that represents a non-avoidable hazard for the island of Tenerife.

Teide and Pico Viejo (TPV) are twin stratovolcanoes situated on the island of Tenerife (Canary Islands) that constitute one of the most important active oceanic island volcanic complexes in the world. They started to grow inside the caldera of Las Cañadas less than 200 ka ago and have continued to be active up to the present day, with the last central eruption (Lavas Negras) occurring about 1000 years ago (Carracedo *et al.* 2007).

The activity of this volcanic complex has generated magmas that have evolved from basaltic to phonolitic from 35 ka ago to the present (Martí *et al.* 2008). Most of the products that have been preserved in TPV are thick lava flows of phonolitic composition that crop out at the surface (Ablay & Martí 2000; Carracedo *et al.* 2007), basaltic to intermediate lava flows forming most of the inside of the volcanic edifices (Ablay & Martí 2000; Triebold *et al.* 2006; Martí *et al.* 2008), minor phreatomagmatic deposits of mafic composition (Pérez Torrado *et al.* 2004; Martí *et al.* 2008; García *et al.* 2011) and phonolitic pumice deposits mostly originating from the 2020 a BP eruption of the satellite cone of Montaña Blanca (Ablay *et al.* 1995). This has traditionally led to the assumption that TPV is essentially effusive and so its associated hazard is relatively minor. However, field revisions carried out in recent years (Martí *et al.* 2008; García *et al.* 2011, 2012) have revealed that the amount of explosive volcanism associated with TPV is much greater than was once thought. This led Martí *et al.* (2011) to reconsider the threat that this active volcanic complex represents for the island of Tenerife and to analyse the potential explosive scenarios that could presumably develop in the near future.

We studied the most recent explosive episodes preserved in the geological record of TPV to better characterize them, thereby improving the evaluation of the potential for future explosive episodes and thus enhancing hazard assessment. The lack of continuous outcrops, owing to the erosion of the deposits, and the apparent similarity of most of these deposits mean that stratigraphic correlation and the determination of the relative ages of these outcrops is not a straightforward task. Therefore, in addition to field and laboratory volcanology work, we also undertook a detailed petrological and geochemical study including mineral chemistry to identify possible fingerprints that would establish a precise correlation between these deposits and determine their relative stratigraphy. In this paper we describe the relative stratigraphy of the deposits, their petrological and geochemical characteristics, and the correlations between these deposits and their potential vents, and, finally, we highlight the relevance of explosive volcanism in hazard assessment of the Teide–Pico Viejo complex.

Geological background

The TPV complex consists of two stratovolcanoes and several flank vents, which started to grow simultaneously within the caldera of Las Cañadas around 180–190 ka ago (Fig. 1) (Hausen 1956; Araña *et al.* 1971; Ablay 1997; Ablay *et al.* 1998; Ancochea *et al.* 1999; Ablay & Martí 2000; Carracedo *et al.* 2007). This volcanic depression originated as a result of several vertical collapses of the edifice of Las Cañadas, the former central volcanic edifice on Tenerife (Martí *et al.* 1994, 1997; Martí & Gudmundsson 2000). The TPV complex has a maximum elevation of 3718 m above sea level (a.s.l.) (the summit of Teide) and steeply sloping flanks.

The volcanic stratigraphy of TPV was characterized by Ablay & Martí (2000) on the basis of a detailed field and petrological study. Subsequently, Carracedo *et al.* (2003, 2007) provided the first group of isotopic ages from TPV products. The eruptive history of the TPV complex consists of a main eruption period characterized by mafic to intermediate lavas that form the core of these stratovolcanoes and filled in most of the depression of Las Cañadas and the adjacent La Orotava and Icod valleys. Phonolitic eruptions predominated from 35 ka ago onwards and their products today cover the volcanoes' flanks and the infill sequence of the Icod Valley and part of La Orotava Valley (Ablay *et al.* 1998; Ablay & Martí 2000; Martí *et al.* 2008).

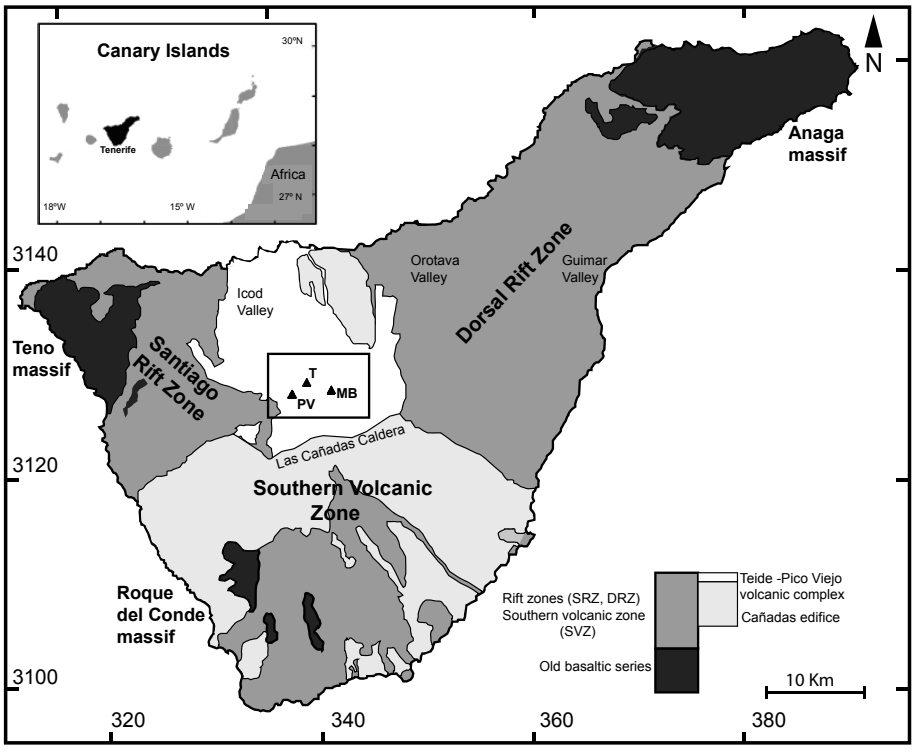

Fig. 1. Location of the Canary Islands and Tenerife. Simplified geology and stratigraphy of Tenerife. Main vents are shown as black triangles: T, Teide; PV, Pico Viejo; MB, Montaña Blanca.

Phonolitic eruptions from TPV have occurred both from the central vents and from a number of satellite vents distributed on the flanks. These flank vents have generated both effusive (i.e. lava flows and domes) and explosive eruptions, ranging in size from 0.01 to >1 km^3 dense rock equivalent (DRE). Effusive eruptions occurred during the whole period of phonolitic volcanism and generated thick lava flows and domes. Explosive eruptions were mostly concentrated in the Holocene (Table 1) and caused extensive pumice fall deposits and pyroclastic density currents (PDCs), some of which have been associated with dome and lava-flow gravitational collapses during sub-Plinian to Plinian eruptions (Martí *et al.* 2008, 2011; García *et al.* 2011). Each of these eruptive centres is associated with a single eruption in which several phases can be distinguished (Ablay & Martí 2000).

Methods

Field reconnaissance was conducted to identify and characterize the various TPV pyroclastic deposits and to locate their possible vents and establish their relative stratigraphy. Description of outcrops (Figs 2 and 3; see also Table 1) defined the stratigraphic positions of the deposits and the study of the macroscopic textural and mineralogical characteristics of components' variations in grain size and thickness, and macroscopic component analysis. Fieldwork also included sample collection for subsequent geochemical and mineralogical analysis with the aim of identifying fingerprints that would confirm stratigraphic correlations.

The mineralogical and geochemical analyses of the studied samples were performed only for correlative purposes given that a more detailed petrological and petrogenetic study was beyond the scope of this work. Our working hypothesis, based on previous petrological studies of TPV rocks (Ablay *et al.* 1997; Wiesmaier *et al.* 2011; Andújar *et al.* 2013), was that products from the same eruption would have relatively homogeneous mineralogical and geochemical compositions, distinct from the products of other eruptions. Whole-rock analyses of 67 samples from various outcrops were performed by the GeoAnalytical Laboratory at Washington State University using its X-ray fluorescence (XRF) and inductively coupled plasma mass spectrometry (ICP-MS) facilities (Table 2). The relative error of the measurement was less than 1% for the major and trace elements using the XRF method, and with the ICP-MS method was less than 5% for the REE and less than 10% for the remaining trace elements.

Mineral compositions were determined using an electron microprobe (Cameca SX-50, Serveis Científic-Tècnics, University of Barcelona) with an accelerating voltage of 20 kV. The sample current was 6 nA for glasses and 15 nA for minerals, and the beam size was 1 μm for minerals and 10 μm for glasses. Although Na was analysed initially for only 20 s to minimize loss, the peak counting times for the other elements were 10 s.

The charcoal found in association with three pumice units was analysed by accelerator mass spectroscopy (AMS) by Beta Analytic Inc. (Miami, FL, USA) to study its carbon isotopic composition. These samples were taken from different parts of the study area. A charcoal sample underneath the TPV North Flank unit (see below) and above a palaeosoil was located at 3132612N, 336669W; 4 g of the sample (laboratory number Beta-301363) were taken and an age of 1790 ± 30 a BP was determined using the IntCal04 calibration curve (Reimer *et al.* 2004) (conventional radiocarbon age 1770 ± 30 a BP, intercept of radiocarbon age with calibration 710 BC to AD 240). Sample RB1 was from the Boquerón deposit and yielded an age of 5630 ± 60 a BP (García *et al.* 2012). The final charcoal sample belongs to the Llanos de la Santidad unit (laboratory number Beta-293009). It was found at the top of the pumice deposit and below an altered scoria unit cropping out in the south of the study area, and yielded an age of 3520 ± 30 a BP (conventional radiocarbon age 3540 ± 30 a BP was calculated using an assumed delta ratio of ^{13}C, and intercept of radiocarbon age with calibration curve of 1890 BC to 3840 BP).

Table 1. *Summary of the phenocryst characteristics in the pumice deposits studied*

Unit	Phenocrystal %	Feldspars		Biotite		Clinopyroxene		Fe–Ti oxides		Microlites (<100 μm)	Vesicularity		
		%	Size (max.)	%	Size (max.)	%	Size (max.)	%	Size (max.)		Size (mm)	%	Shape
Llanos de la Santidad	0.5–0.1	12	500 μm	80	300 μm	–	–	8	200 μm	Bt, Kfsp	3	45	R, E
Mtñ. Blanca	0.5–0.1	80	2 mm	–	–	20	600 μm	–	–	Kfsp, cpx	5	48	R, E
Mtñ. Majua	1.0–3.0	65	2 mm	25	<1 mm	7	200 μm	3	500 μm	Kfsp, cpx	5	47	E
Gemelos	1.0–3.0	85	2 mm	5	200 μm	5	600 μm	5	500 μm	Kfsp, bt	500 μm	35	R
Boquerón	3.0	70	1 mm	15	200 μm	10	200 μm	5	400 μm	Kfsp, bt	5	45	E, A, R
Hoya Abrunco, fallout	0.5–0.1	–	–	50	2 mm	40	1 mm	10	200 μm	Kfsp, bt	6	52	E, A, R
Hoya Abrunco, PDC	0.5–0.1	5	200 μm	10	200 μm	80	500 μm	5	200 μm	Kfsp, bt, cpx	3	54	E, A, R
Pico Cabras	<0.5	–	–	–	–	–	–	–	–	Kfsp, bt	<100/1	53	R, E
TPV North Flank	<0.5	–	–	–	–	–	–	–	–	–	>250/500	52	R, E
Roques Blancos	<0.5	100	1 mm	–	–	–	–	–	–	–	>250/500	52	R, E
Calderón, Unit I	1.0–3.0	50	<2 mm	–	–	40	1 mm	10		Kfsp, cpx	5	48	R
Calderón, Unit II	<0.5	–	–	–	–	80	1 mm	20	<200 μm		200 μm	42	R

Vesicle shapes: R, rounded; E, elongated; A, amoeboid.

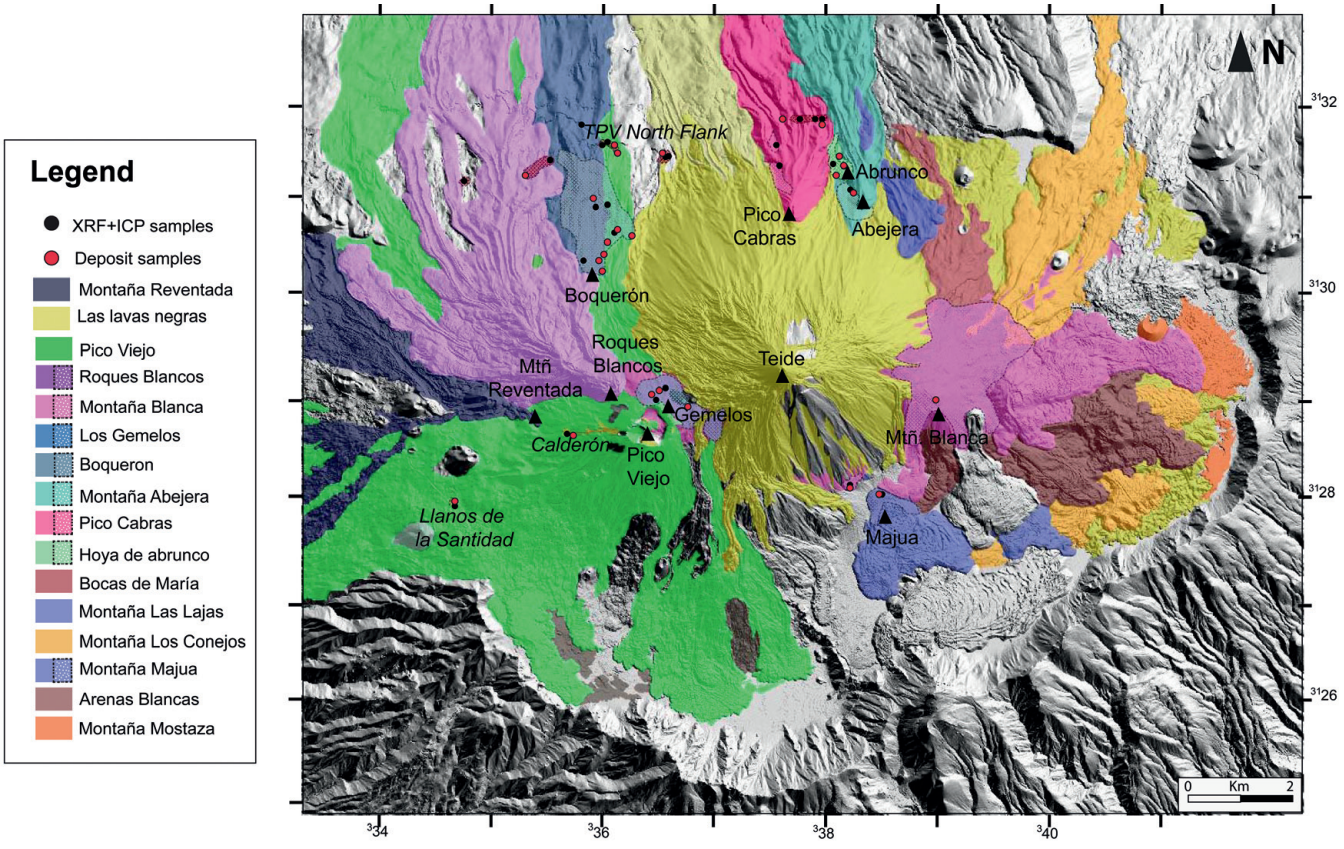

Fig. 2. Simplified geological map of the Teide–Pico Viejo complex (modified from Ablay & Martí 2000) showing the central and flank Holocene eruptions of felsic and hybrid compositions. Geochronological data are from Carracedo *et al.* (2007). Main vents are shown as black triangles. The studied deposits and the corresponding samples are indicated by red circles; XRF and ICP-MS analysed samples are indicated with black circles; analyses are shown in Table 2. The pumice deposits associated with the main flanks of the volcanoes of TPV are indicated by the stippled pattern (projection: UTM 28N).

Table 2. *Whole-rock analyses of pumice deposits in Teide–Pico Viejo volcanic complex (unnormalized major elements (weight %) and unnormalized trace elements (ppm))*

Unit:	Boquerón					Pico Cabras			Calderón		Abejera
Sample:	P.U.L	B.H11	B.RT	B.RTJ1	B.RTJ2	PC.H4	P.CABRAS.C	PC-1	CALD.N.1	CALD.N.3	M.A.P
Latitude (N):	3132795	3131111	3131660	3131613	3131613	3132399	3133287	3132788	3127300	3127300	3131919
Longitude (E):	335411	335636	335487	335290	335290	338793	339622	338715	334745	334745	340144
SiO_2	57.44	57.31	58.44	56.84	57.01	57.92	58.91	58.63	56.25	58.89	56.72
TiO_2	0.687	0.679	0.628	0.696	0.694	0.662	0.633	0.628	1.129	0.760	0.776
Al_2O_3	19.43	19.44	18.90	19.43	19.28	19.10	18.89	18.90	19.63	19.06	19.67
FeO*	3.40	3.35	3.51	3.41	3.41	3.58	3.50	3.49	4.52	3.68	3.92
MnO	0.196	0.189	0.195	0.185	0.181	0.199	0.197	0.198	0.177	0.189	0.193
MgO	0.37	0.38	0.34	0.38	0.40	0.38	0.32	0.35	0.89	0.49	0.45
CaO	0.80	0.78	0.75	0.83	0.84	0.77	0.74	0.74	2.05	1.03	0.94
Na_2O	8.53	8.76	9.07	8.34	8.53	8.83	9.18	9.26	8.66	9.34	8.23
K_2O	5.14	5.23	5.42	5.02	5.08	5.30	5.45	5.46	4.76	5.36	4.93
P_2O_5	0.097	0.083	0.081	0.100	0.093	0.094	0.084	0.083	0.267	0.125	0.142
Sum	96.09	96.20	97.33	95.23	95.52	96.82	97.92	97.74	98.31	98.92	95.96
LOI (%)	3.79	2.92	2.35	4.11	3.64	2.21	1.94	1.63	0.99	1.24	3.97
Ni	3	2	3	3	2	3	3	3	5	3	3
Cr	1	2	2	3	3	4	2	4	0	1	4
Sc	1	0	1	1	2	1	2	2	1	2	2
V	15	14	8	14	17	13	7	9	18	16	18
Ba	113	94	24	135	129	47	26	29	1393	134	134
Rb	170	173	170	165	169	166	171	168	134	163	155
Sr	16	15	7	19	26	12	7	5	426	77	61
Zr	1047	1024	989	1031	1025	985	992	991	759	934	991
Y	37	37	38	37	37	37	38	38	35	36	35
Nb	236	231	225	234	232	225	226	226	199	217	226
Ga	28	30	29	28	29	29	29	28	27	28	28
Cu	2	1	1	2	1	1	2	2	3	3	3
Zn	118	121	125	114	114	127	126	126	114	123	122
Pb	21	21	20	20	20	20	20	20	20	18	20
La	112	106	112	108	108	110	108	110	105	108	105
Ce	191	193	186	192	191	188	187	189	181	186	184
Th	31	30	28	31	31	28	28	29	25	26	29
Nd	58	55	56	56	56	55	54	57	58	54	55
U	8	8	8	8	7	6	8	6	6	8	7

Stratigraphy

The stratigraphic reconstruction, along with the variations in thickness and grain size established during the fieldwork, allowed the identification of several pyroclastic deposits at different sites and stratigraphic positions (Figs 2 and 3). Although some deposits were clearly associated with vents located on the flanks of TPV, the source vent of others remains unknown. The flank vents on TPV represent an episode of felsic activity that produced about $1.7 \pm 0.5\,km^3$ of phonolitic products from at least 10 satellite vents. These vents are located mostly on the NW, north, east and SE flanks of TPV between 2200 and 2600 m a.s.l. and include (in clockwise order) Roques Blancos, El Boquerón, Pico Cabras, Hoya del Abrunco, Montaña Las Lajas, Bocas de Marie, Montaña Blanca, Los Roquillos, Montaña Majua and Montaña de la Cruz (Fig. 2). The flank vents situated in the caldera of Las Cañadas that emitted only mafic magmas were not considered to be part of the TPV complex (Ablay & Martí 2000) given that they are associated with the activity of the rift systems.

For practical purposes, we separated the TPV pumice outcrops into two main groups on the basis of their known or unknown potential vent sources: the pumice deposits that in the field could be traced to known vents were Abejera, Abrunco, Pico Cabras, El Boquerón, Montaña Majua, Montaña Blanca, Roques Blancos and Los Gemelos, and the samples with unknown vents were named TPV North Flank, Llanos de la Santidad and Calderón.

On the north flank of Teide between Abrunco and Pico Cabras (Fig. 2) there is a phonolitic pumice cone, *c*. 900 m in diameter and breached by the emplacement of a phonolitic lava flow around 200 m to the west. This flow covers part of the pumice cone corresponding to Abrunco, the oldest vent on the north flank of TPV (García *et al.* 2011). Associated with this eruption there is a PDC deposit covered by a pyroclastic deposit originating from the same eruption (García *et al.* 2011). This fallout deposit is composed of well-sorted, yellow to grey angular lapilli pumice, with a few obsidian lithic fragments (Fig. 3). The distal deposits have mostly been eroded out but in proximal areas may be up to 2 m in thickness. The PDC deposit is fairly heterogeneous and poorly exposed and has different lithofacies at the various outcrops (see García *et al.* 2011). This deposit overlies a clastogenic lava flow that was locally eroded by the pyroclastic current during its emplacement.

Other pumice deposits found on the north flank of Teide are associated with the Pico Cabras and Abejera domes (Fig. 2). These are two volumetrically significant vent complexes whose lava-flow products extend into the Icod Valley and almost reach the northern

Table 2. *(Continued)*

Unit:	TPV North Flank						Montaña Blanca	Llanos de la Santidad	Gemelos		Majua		Abrunco	
Sample:	P.1600ANL4	P.1600ANL5	ROQ.BLAN.6	ROQ.BLAN.7	ROQ.BLAN.8	P1600.32	MTNBLANCA	ICS	Gemelos2	GEMELOS3	M.M.1	M.M.2	PDC	Fallout
Latitude (N):	3132612	3132838	3132503	3132085	3133164	3132532	3128019	3125928	3127941	3128168	3126130	3126170	3132411	3132228
Longitude (E):	336669	335519	334423	332773	335025	336600	341702	332586	336413	336595	340736	340144	339798	334002
SiO_2	57.79	58.35	58.11	57.97	57.99	58.64	58.35	57.36	58.95	58.82	55.69	58.45	59.68	58.80
TiO_2	0.647	0.625	0.632	0.627	0.638	0.628	0.623	0.780	0.660	0.644	0.883	0.692	0.767	0.764
Al_2O_3	19.01	18.73	19.00	18.72	19.02	18.81	19.19	19.39	19.17	19.42	20.01	19.13	18.95	18.82
FeO*	3.53	3.37	3.48	3.55	3.57	3.45	3.53	3.07	3.63	3.58	3.84	3.28	3.06	2.98
MnO	0.198	0.196	0.193	0.195	0.197	0.197	0.200	0.166	0.190	0.201	0.191	0.191	0.167	0.167
MgO	0.35	0.34	0.34	0.33	0.34	0.33	0.31	0.43	0.38	0.32	0.58	0.38	0.44	0.44
CaO	0.77	0.74	0.78	0.76	0.74	0.74	0.71	0.91	0.76	0.72	0.96	0.79	0.86	0.86
Na_2O	8.90	8.97	8.94	8.97	8.80	9.09	9.41	7.42	9.30	9.49	7.54	8.81	9.05	8.55
K_2O	5.31	5.40	5.30	5.35	5.33	5.47	5.41	4.84	5.40	5.42	4.65	5.41	5.32	5.26
P_2O_5	0.100	0.083	0.079	0.085	0.092	0.083	0.072	0.128	0.081	0.076	0.168	0.105	0.108	0.104
Sum	96.61	96.82	96.87	96.55	96.72	97.44	97.79	94.48	98.54	98.67	94.52	97.22	98.39	96.74
LOI (%)	2.63	2.45	2.40	2.29	2.93	2.14	1.85	4.77	1.47	1.37	4.27	2.81	1.55	2.37
Ni	3	3	2	4	3	3	3	3	3	2	6	3	2	2
Cr	2	1	2	1	2	2	2	3	5	1	6	1	2	1
Sc	1	1	0	1	1	1	0	1	1	0	0	1	0	2
V	9	12	9	10	11	9	7	18	12	12	25	12	18	20
Ba	37	28	26	24	40	26	16	559	52	26	416	102	570	563
Rb	165	168	167	169	169	171	179	150	174	174	145	175	154	153
Sr	13	7	7	7	8	4	3	36	14	6	72	10	17	17
Zr	991	979	991	984	1001	991	1065	858	1023	1059	922	1007	837	828
Y	38	37	38	37	36	37	39	30	39	40	36	37	30	29
Nb	225	223	226	225	226	226	242	190	234	242	207	228	185	184
Ga	29	29	30	29	30	30	31	26	29	30	27	29	27	26
Cu	2	1	5	1	2	2	1	0	3	2	5	2	1	0
Zn	125	124	123	123	124	129	131	99	127	130	119	122	107	106
Pb	21	20	19	21	20	20	22	17	21	23	19	20	16	17
La	111	105	111	105	106	111	112	97	110	118	106	107	94	94
Ce	191	191	190	188	186	190	198	162	193	199	189	188	163	163
Th	29	28	28	28	29	28	32	25	30	32	28	29	25	25
Nd	57	56	58	57	55	56	60	46	57	60	57	57	48	49
U	8	7	6	7	9	7	8	7	8	10	8	8	7	7

LOI, loss on ignition.

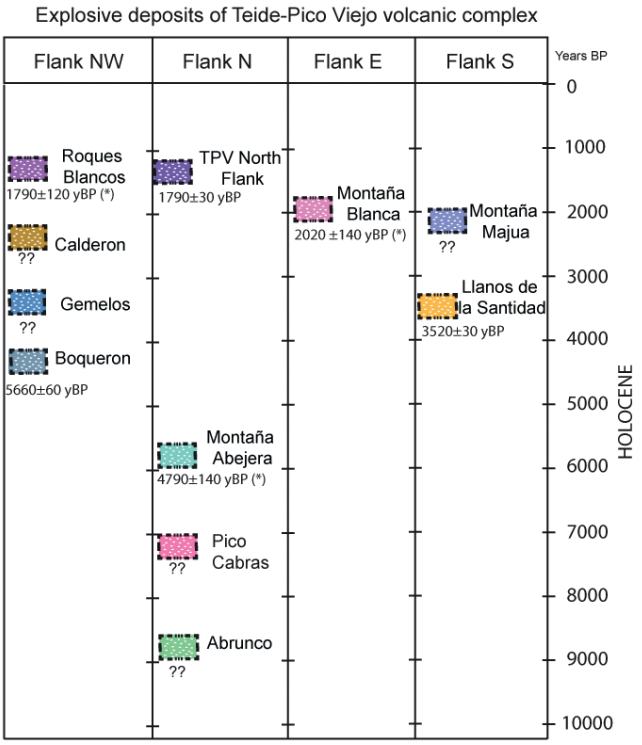

Fig. 3. Age of the Holocene pumice fallout deposit of the NW, north, east and south flanks of the Teide–Pico Viejo volcanic complex. Geochronological data from (*)Carracedo *et al.* (2007) and García *et al.* (2011). The legend colours agree with those of the map in Figure 2.

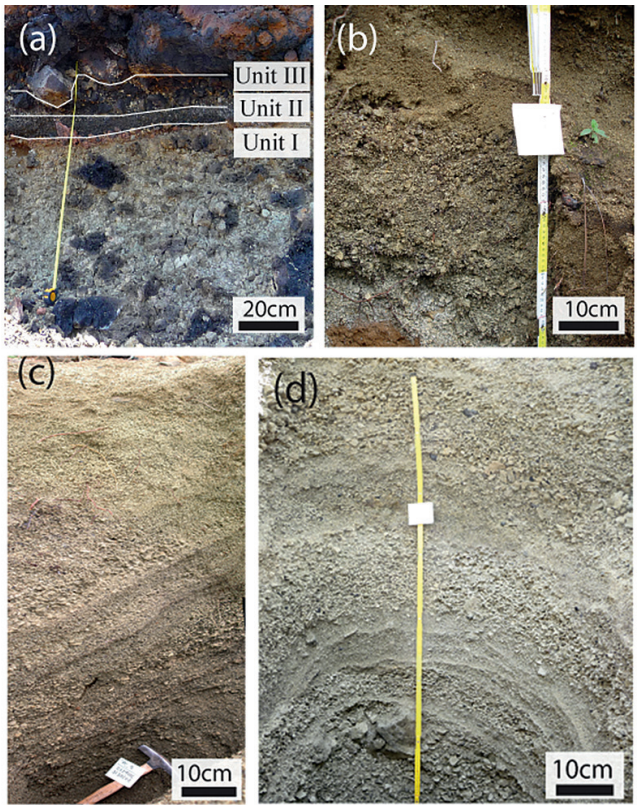

Fig. 4. Examples of pumice fallout deposits from different vents. (**a**) Calderón deposit, Units I, II and III; (**b**) TPV North Flank deposit; (**c**) Pico Cabras deposit; (**d**) Abrunco fallout deposit.

coast of Tenerife. Abejera is the younger of these two domes and consists of two vents that produced three blocky lava flows of evolved phonolite with a DRE volume of *c.* 0.36 km^3 (Ablay & Martí 2000). Abejera also includes a partially reworked fallout deposit (Fig. 3), a few centimetres thick in proximal areas, formed of subrounded to rounded, poorly vesiculated lapilli pumice and a few obsidian lithic fragments (4 vol%). On the other hand, Pico Cabras emitted an important lava flow (0.28 km^3 DRE volume) and a few well-preserved, locally reworked outcrops of well-sorted, green to grey subangular lapilli pumice, with stratification. Proximal deposits are up to 2 m in thickness (Fig. 3). However, we found no stratigraphic indicators that could be used to correlate single layers in the different outcrops and so we describe the Pico Cabras pumice deposits as a single unit.

El Boquerón is a dome complex located on the northwestern flank of the Pico Viejo stratovolcano close to the Roques Blancos dome complex (Fig. 2). The final eruption of El Boquerón occurred 5600 a BP (García *et al.* 2012) and generated a widely dispersed pumice fall deposit and 0.04 km^3 of lava flows, which flowed down into the Icod Valley. As in the case of the Montaña Blanca pumice, El Boquerón has been interpreted as being the result of a sub-Plinian eruption with a mass eruption rate (MER) of (6.9–8.2) $\times 10^5$ kg s^{-1}, DRE volume of (4–6) $\times 10^7$ m^3 and a 9 km high eruption column (García *et al.* 2012). The pumice deposit is poorly preserved and has poor exposure. It corresponds to a well-sorted deposit composed of non-welded, micro-vesicular, angular to subangular, yellow to grey lapilli pumice with subordinate lithic clasts of obsidian and phonolitic lavas.

An extensive pumice fallout field lies on the shoulder between the edifices of El Teide and Pico Viejo and has been associated with the phonolitic domes of Los Gemelos (Ablay *et al.* 1995). This field consists of well-sorted, bedded, angular, pale green pumice lapilli fallout deposits, grading upwards locally into densely welded spatter, with a high content of juvenile lithic clasts of obsidian and lavas. Inside the caldera of Las Cañadas at the bottom of the Teide volcano, there is a pumice fallout deposit associated with Montaña Majua, a denuded pumice cone of *c.* 700 m in diameter breached to the SE by the emplacement of a thick lobate phonolite lava flow (*c.* 0.03 ± 0.01 km^3). This pumice fallout deposit is a single, well-sorted, reversely graded deposit formed by non-welded angular pumice lapilli with a low content of juvenile obsidian and oxidized lithic fragments of lava. Proximal exposures reveal crude, centimetre-scale stratification and the development of crystal-rich layers in the basal portions. Distal localities are unstratified. This deposit was classified as Strombolian on the basis of dispersal criteria (Ablay 1997; Ablay & Martí 2000). Part of the Montaña Majua pumice deposits covers part of the slopes of Teide, 0.6–1.2 km to the NW.

The largest fallout deposit is associated with the products of a substantial explosive eruption that occurred on Montaña Blanca on the eastern side of Teide (Fig. 2). This deposit corresponds to an intermediate phase of the Montaña Blanca eruption that occurred about 2 ka ago and generated phonolitic domes and lava flows (Ablay *et al.* 1995). This fallout deposit contains well-sorted, pale and angular pumice with some concentration of lithic fragments of obsidian and lavas. In proximal areas on Montaña Blanca the top of this deposit corresponds to a welded fallout facies consisting of flow-banded, poorly vesiculated obsidian with a relict clastic texture, supporting poorly inflated angular pumice. This pumice fall deposit was interpreted as deriving from a sub-Plinian phase from the main vent at Montaña Blanca that formed a 9 km high eruption column (Ablay *et al.* 1995; Folch & Felpeto 2005).

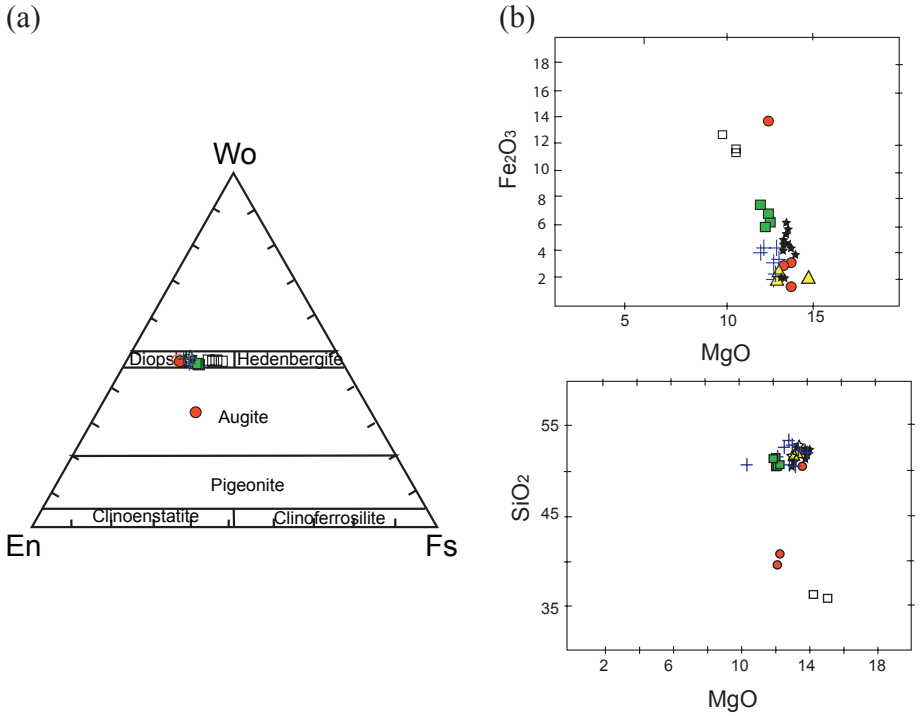

Fig. 5. (**a**) Classification diagram of clinopyroxenes (Morimoto 1988) from the TPV pumice deposits. Clinopyroxenes are classified using the total number of cations on a six-oxygen basis; the Fe_2O_3 was estimated according to the method used by Droop (1987). Filled circle, Calderón Unit I; open circle, Calderón Unit III; open square, Mtn. Blanca; triangle, Mtn. Majua; cross, El Boquerón; filled square, Los Gemelos; filled star, Abrunco PDC; open star, Abrunco (fallout).
(**b**) Selected correlation diagrams (SiO_2 v. MgO and Fe_2O_3 v. MgO) of core analysis for clinopyroxenes of the TPV pumice deposits.

The dome of Roques Blancos on the northwestern flank of Pico Viejo (Fig. 2) consists of two vents (Balcells & Hernández Pacheco 1989), both of phonolitic composition. Roques Blancos is the most voluminous ($0.83 \pm 0.1\ km^3$) of the compound phonolite lava flows that erupted from the parasitic fissure vents on TPV. It covers an area of $18 \pm 2\ km^2$, extending down the north flank of Pico Viejo and filling in the Icod Valley (Ablay & Martí 2000; Martí *et al.* 2011). There is a pyroclastic succession associated with Roques Blancos that consists of a lapilli-size pumice fall deposit up to 65 cm thick characterized by poor exposure, with proximal outcrops with a stratified, inversely graded pumice deposit formed by non-welded, micro-vesiculated, angular to subangular lapilli pumice, with a low (>2 wt%) content of lithic clasts (obsidian and lava fragments). This deposit is discontinuously distributed along the northwestern flank of TPV (Fig. 2).

The Llano de la Santidad deposit is found within the caldera of Las Cañadas, inside the Ucanca depression (Fig. 2). This deposit overlies an older lava flow and consists of a 1.7 m thick yellow, angular, highly vesicular fine lapilli pumice, unconformably overlain by a 40 cm thick red scoria deposit. Between the red scoria deposit and the pumice deposit we found charcoal fragments that yielded a ^{14}C age of 3450 ± 30 a BP.

Another pumice deposit that is widely distributed on the northern flank of the TPV complex, in particular along the road that runs east–west at an altitude of 1600 m a.s.l. (Figs 2 and 3), consists of a series of dispersed outcrops of pumice fall deposits of unknown provenance. All of these outcrops have similar lithological, textural and compositional characteristics and so we grouped them as a single deposit (the TPV North Flank deposit, given that most of the deposits crop out on the north flank). Some of these outcrops situated on the eastern side of TPV (Fig. 2) overlie the Pico Cabras lava flow, whereas towards the west they are located between the Roques Blancos lava flows, as described above. This pyroclastic deposit consists of well-stratified, inversely graded, subangular, grey to yellow, highly vesicular fine lapilli pumice, with a few lithic obsidian clasts (>2 wt%), reaching a maximum thickness of 65 cm (Fig. 4). Charcoal fragments found in a dark brown soil at the base of this deposit yielded an age of 1770 ± 80 a BP, the same age as Carracedo *et al.* (2003, 2007) attributed to the Roques Blancos dome.

Inside El Calderón subsidence structure we identified a succession of pumice fallout deposits (Figs 2 and 3), the source of which remains unknown. El Calderón consists of an asymmetric, circular collapse structure, 30 m in diameter and with a depth of 4 m in its shallowest part and around 15 m in the deepest part (e.g. Araña *et al.* 1989; Ablay & Martí 2000). On the walls of this depression a succession of three pyroclastic units is exposed with a maximum thickness of 77 cm and a 3 m covering of clastogenic lava from Cuevas Negras (Carracedo *et al.* 2007). From top to bottom we distinguished the following units: Unit III, formed of 17 cm of unsorted grey pumice clasts, with variable grain size from lapilli to bomb; Unit II, formed of 15 cm of well-sorted dark grey mafic scoria clasts with lava fragments (6 vol%); Unit I, formed of a 47 cm thick layer of non-sorted lapilli to bomb pumice, yellow to grey in colour, with highly elongated vesicles, lithic clasts of lavas and obsidian (10 vol%), with its upper 5–8 cm consisting of a red, welded pumice layer.

Petrology and geochemistry

Petrographic characteristics

Representative randomly collected pumice samples from all recognized pyroclastic units from each deposit were examined. All of the studied juvenile lapilli pumice samples were microvesicular, glassy and phenocryst poor, and in some cases had a total lack of phenocrysts (i.e. Roques Blancos).

Phenocryst phases (Table 1) are represented by feldspar (Kfsp, Plg), clinopyroxene (Cpx), biotite (Bt), titanomagnetite (Ttn-Mag) and ilmenite (Ilm); the phenocryst content in the deposits varies between <0.5 vol% in Pico Cabras and TPV North Flank and 3 vol% in El Boquerón. Feldspar was the most common type of phenocryst found and was euhedral to subhedral, with a maximum size of 2 mm and an average size of 0.5 mm. Microlites (<100 μm) were found in all deposits except in Pico Cabras, El Calderón Unit III and Abrunco,

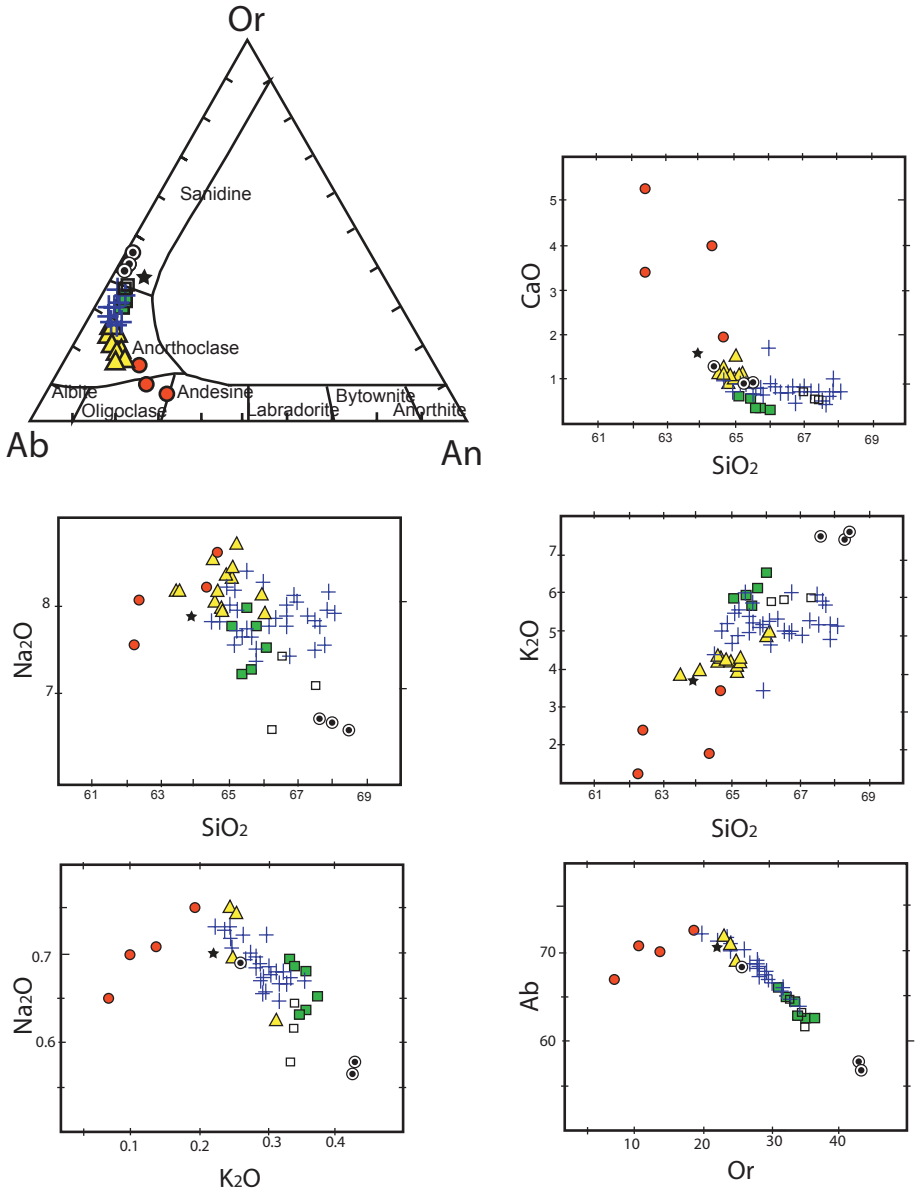

Fig. 6. Classification diagram of the feldspar (Ab–An–Or) TPV pumice deposit. The formula composition was calculated on an eight-oxygen basis following the method described by Deer *et al.* (1992). Major element diagrams of the feldspar core analyses: SiO_2 v. K_2O, Na_2O and CaO_2; Na_2O v. K_2O; Ab v. Or. Filled circle, Calderón Unit I; open square, Mtn. Blanca; double circle, TPV North Flank deposit; cross, El Boquerón; filled square, Los Gemelos; filled star, Abrunco PDC; open star, Abrunco (fallout)

where the microlite content was very low. Clinopyroxene was less abundant, with an average size of 0.65 mm and a maximum size of 2 mm. Biotite was present in the pumice samples (elongate and rectangular shapes) as phenocrysts of around 1 mm and as microlites in the groundmass (<100 μm). Fe–Ti oxides were the least abundant minerals and were always relatively small (around 500–200 μm).

Pumice clasts were moderately to poorly vesicular and had heterogeneous textures that varied in terms of their degree of vesicularity and crystallinity. Vesicles ranged in size from a few millimetres to few micrometres and in shape from spherical to elongate or flat. The thickness of the vesicle walls ranged from a few to tens of micrometres, suggesting the occurrence of high nucleation rates and an expansion-dominated coalescence (Szramek *et al.* 2006). Vesicles were usually preserved, although a few amygdales replenished by secondary mineralization by calcite and, more rarely, by barite were also identified.

In deposits such as those at El Boquerón, El Abrunco and Los Gemelos groundmass crystallinity varies at specimen scale and is correlated with the degree of vesicularity: microlite-poor areas (5 vol% of microlites) are also vesicle-poor, with only small round vesicles; microlite-rich areas (50 vol% of microlites) have vesicularity up to 45 vol%. This relationship between vesicles and groundmass crystallinity is probably due to the effects of post-fragmentation expansion or even to clast recycling during less explosive phases (see Wright *et al.* 2006). Microlites consist of acicular sanidine with length along the major axis ranging between 200 and 10 μm, as well as elongated biotite with major axis length of around 200 and 20 μm. Clinopyroxenes were less frequent microlites than sanidine microlites and of different shapes (elongate and rectangular), and ranged in size from 200 to 10 μm. Occasionally, microlites occurred in small groups in the crystal-rich glass, but more commonly they were found as single crystals. Clasts from incipiently welded facies had highly heterogeneous textures with abrupt variations in vesicle size and spherulitic aggregates.

Mineral chemistry

Microprobe analysis (of phenocrysts and vitric groundmass) was performed on pumice samples from all of the deposits. Clinopyroxene was present in all of the pumice samples except in

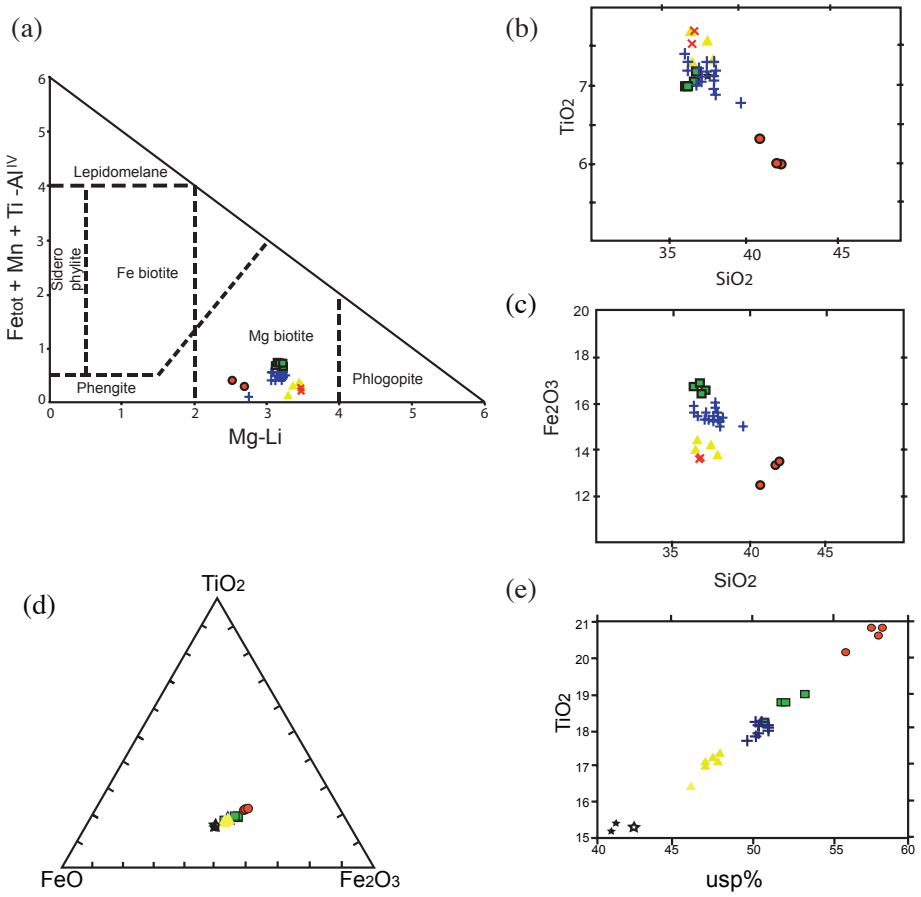

Fig. 7. (**a**) Plot of the studied samples in the classification diagram for micas (Tischendorf 1995). The micas were calculated on a 24-oxygen basis and four OH group following the method described by Deer *et al.* (1992). All of the samples from TPV are classified as Mg-biotite using the classification of Tieschendorf (1997). The estimate for Li_2O is based on Yavurt *et al.* (2001) and the equation Li_2O wt% = 155(MgO) − 3.1, for SiO_2 >34 wt% and MgO >6 wt%. (**b**, **c**) Harker diagrams of biotite analysis: (**c**) SiO_2 v. TiO_2; (**d**) SiO_2 v. Fe_2O_3. (**d**, **e**) Plots of Fe and Ti oxide compositions: (**d**) FeO–TiO_2–Fe_2O_3 diagram; (**e**) Usp% v. TiO_2 diagram. Magnetite and ilmenite formulae were calculated on a four-oxygen basis; the total FeO was recalculated following the method of Carmichael (1967). Triangle, Montaña Majua; ×, Llanos de la Santidad deposit; +, El Boquerón; square, Los Gemelos; circle, Calderón Unit I; filled star, Abrunco PDC; open stars, Abrunco (fallout).

those from TPV North Flank, Roques Blancos, Llanos de la Santidad and Pico Cabras. Following the classification of Morimoto (1988), most of the phenocrysts analysed correspond to diopside ($Wo_{51–46}En_{40–36}Fs_{15–10}$), although El Calderón Units I and III correspond to augite ($Wo_{45–31}En_{44–40}Fs_{25–15}$) (Fig. 5a). Most of the diopside crystals show slight normal and inverse zoning in Mg- and Fe-rich portions. In Figure 5b the variation diagrams of MgO v. Fe_2O_3 and SiO_2 vs. MgO for clinopyroxenes are shown and allow the deposits to be differentiated.

Feldspar phenocrysts occur in all pumice deposits except those of El Calderón Unit III and Pico Cabras; their composition ranges from anorthoclase to sanidine and, exceptionally, oligoclase (El Calderón Unit I) (Fig. 6). Alkali feldspar of sanidine composition was found in the deposits from Montaña Blanca, TPV North Flank and Abrunco but was not as common as anorthoclase, which was found in most of the studied deposits (Los Gemelos, Montaña Majua, Abrunco, Llanos de la Santidad, Montaña Blanca and El Boquerón). Microprobe profile analyses performed on feldspar phenocrysts showed zonation patterns in both the sanidine and the anorthoclase crystals. Analyses of feldspar crystal cores are shown in Figure 6.

All the biotite crystals correspond to Mg- and Ti-rich biotite and were present in the Los Gemelos, El Boquerón, Pico Cabras, Llanos de la Santidad, Montaña Majua and El Calderón Unit I deposits (Fig. 7a). The highest Mg and Ti content was found at Llanos de la Santidad and Montaña Majua (Fig. 7b).

Fe–Ti oxides correspond to spinels (magnetite and ilmenite). Titanomagnetite compositions range from $Ups_{41.95}$ to $Ups_{56.71}$ and vary from one deposit to another: El Boquerón $Usp_{54.58}$, Montaña Majua $Ups_{47.39}$, Los Gemelos $Ups_{52.18}$, Pico Cabras $Ups_{46.75}$, Abrunco PDC $Ups_{42.98}$, Abrunco fall out $Ups_{41.95}$, El Calderón Unit I $Ups_{56.71}$ and Montaña Blanca $Ups_{52.80}$ (Fig. 7c and d). Ilmenite compositions range from $Ilm_{88.58}$ to $Ilm_{93.28}$, with the following values: El Boquerón $Ilm_{93.21}$, Montaña Majua $Ilm_{91.63}$, Los Gemelos $Ilm_{93.28}$ and Abrunco $Ilm_{89.07}$.

Whole-rock geochemistry

Representative whole-rock analyses of the studied pumice deposits are given in Table 3 and Figures 8 and 9. All the pumice samples studied from the TPV succession had a peraluminous (A/CNK >1) phonolitic to trachyphonolitic composition, with a SiO_2 content ranging from 51.21 to 60.56 wt %, and a total alkali content (Na_2O + K_2O) between 10.46 and 15.12 wt %.

These pumice samples show the typical geochemical features of evolution by fractional crystallization, as indicated by the corresponding positive and negative correlations between major and trace elements (Fig. 10) that occur in the TPV phonolitic lavas (Ridley 1970; Araña *et al.* 1989; Andújar *et al.* 2010; Wiesmaier *et al.* 2011).

Trace elements including REE show a similar pattern in all samples (Fig. 10) albeit with some differences in the concentration of Ba, Sr, Ti and P, which are more evident for the samples from El Calderón Unit I, Llanos de la Santidad, Montaña Majua and Abrunco PDC. There is also a slight departure from the general REE pattern in these samples (Fig. 10d–f), showing subtle to absent Eu anomalies.

Discussion

Our detailed field study allowed us to identify a number of new phonolitic pyroclastic deposits associated with the recent eruptive

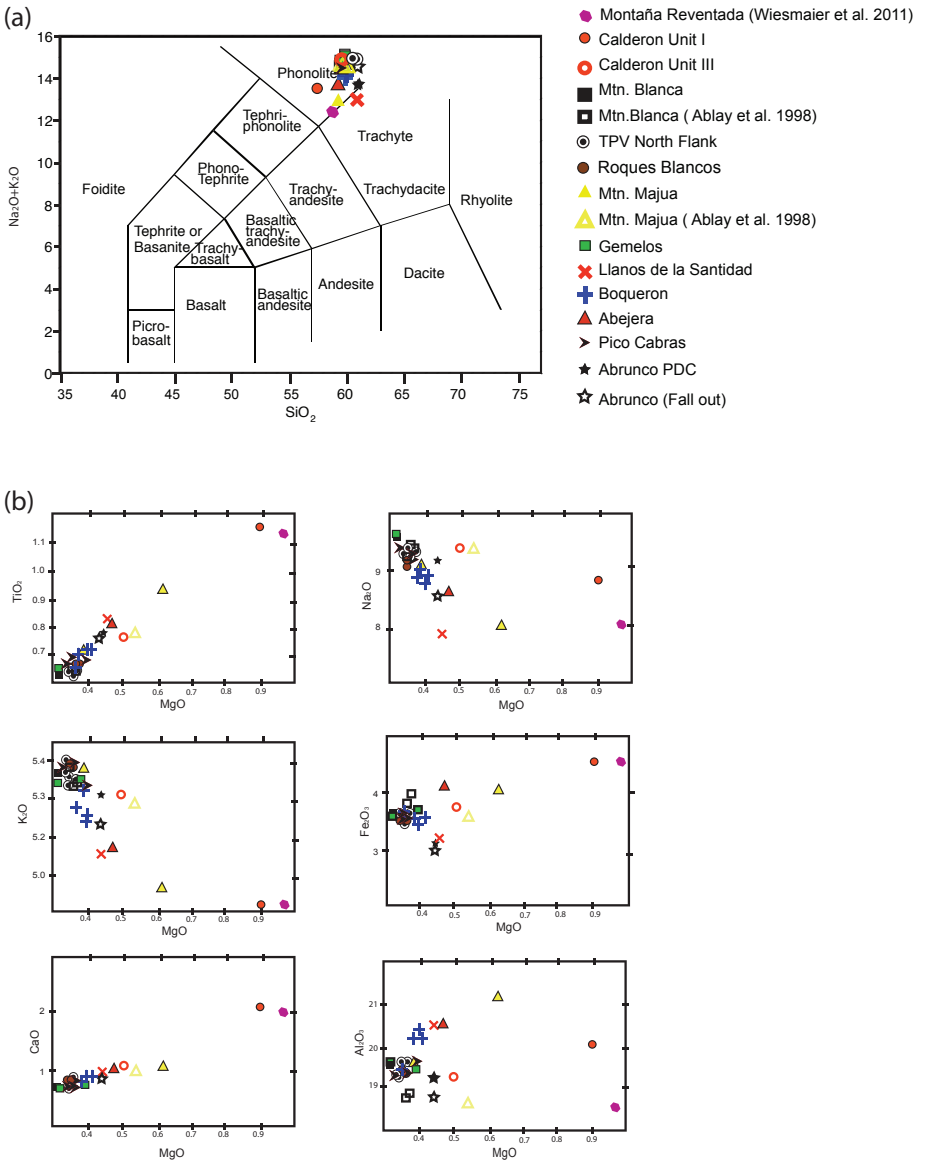

Fig. 8. (**a**) Total alkalis–silica classification diagram (Le Bas *et al.* 1986), including some data from Ablay *et al.* (1998) for comparison. (**b**) Variation of selected major oxides v. MgO (wt%) for TPV pumice deposits. Three analyses from Montaña Blanca and Montaña Majua by Ablay *et al.* (1998) have been included.

history of the TPV complex. Although some of the pyroclastic deposits identified in this study can be clearly correlated in the field with their corresponding vents located on the flanks of the Teide and Pico Viejo stratovolcanoes, others are of unknown origin. The use of existing stratigraphic (Ablay & Martí 2000; Carracedo *et al.* 2007) and geochronological (Carracedo *et al.* 2007) data from the TPV complex and comparisons with the new field data allowed us to establish the stratigraphy of these pyroclastic deposits, which all date from the Holocene.

According to the stratigraphic relationships, the TPV North Flank pumice deposit could be related either to Roques Blancos or, less confidently, to Pico Cabras. This deposit overlies the lavas from these two eruptions but is closest to the pumices from Roques Blancos in terms of its geochemical and petrological characteristics. Moreover, Pico Cabras dates from more than 5911 a BP (see Figs 3 and 4) and so cannot be related to Roques Blancos. In fact, this latter eruption dates from 1714 a BP (Carracedo *et al.* 2007), which is similar to the age we obtained for the TPV North Flank deposits (1770±80 a BP) (see Fig. 4). Therefore, we propose that the TPV North Flank pumice deposit is a distal facies of the Roques Blancos eruption.

The other two deposits of unknown origin, Llanos de la Santidad and El Calderón, could not be correlated to any known vent area using either field stratigraphic criteria or a mineralogical or geochemical basis. In the case of the deposits in El Calderón, the absence of stratigraphic discontinuities in Units I, II and III suggests that these three units were deposited continuously, although their source is unknown (Fig. 3). The difference in composition between Unit II (mafic) and the other units (phonolitic) and the absence of any evidence of mixing in the felsic units suggest that the intermediate layer has a different provenance. It is possible that the two eruptions took place at the same time, with Unit II originating from the northwestern rift zone and Units I and III from the TPV complex. This is not unusual in either the TPV record or the pre-TPV Las Cañadas edifice (Ablay & Martí 2000; Edgar *et al.* 2007). However, we failed to find any evidence that could correlate the units in El Calderón with any specific eruption or vent site. Another possibility would be to associate the sequence at El Calderón with a single eruption generating both mafic and felsic magmas. A more recent example of this type of eruption is the Montaña Reventada, a young flank eruption developed from a fissure vent system on the western flank of Pico Viejo. It generated a composite lava flow consisting of lower basanite and upper trachyphonolite units.

The Llanos de La Santidad deposits found in the interior of the Ucanca depression in the caldera of Las Cañadas cannot be clearly

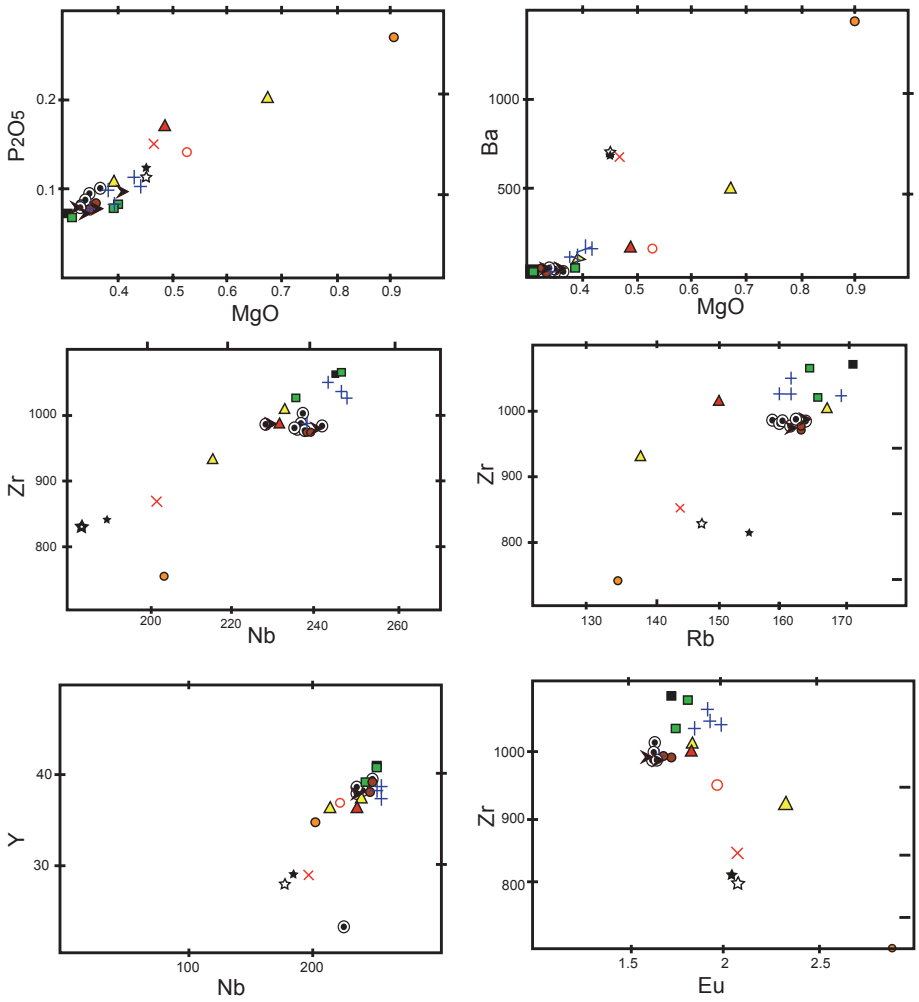

Fig. 9. Variation diagrams of selected trace elements v. MgO and Zr (wt%) for TPV pumice deposits. Filled circles, Calderón Unit I; open circles, Calderón Unit III; black square, Montaña Blanca; double circle, TPV North Flank deposit; filled circle, Roques Blancos; open triangle, Montaña Majua; square, Los Gemelos; ×, Llanos de la Santidad deposit; +, El Boquerón; filled triangle, Abejera deposit; arrows, Pico Cabras; filled star, Abrunco PDC; open star, Abrunco (fallout).

correlated to any known vent. The similar biotite composition in the Llanos de La Santidad and Montaña Majua deposits (Fig. 7e and d, respectively) suggests that these deposits have a common origin. This genetic relationship is also suggested by the similar patterns in the trace elements and REE present in both deposits (Fig. 10). However, the Montaña Majua deposits disperse SE from the vent (Ablay *et al.* 1995; Ablay & Martí 2000), thus making any correlation with the Llanos de La Santidad deposit located to the west unlikely (Fig. 2). Although the deposits at Montaña Blanca, Los Gemelos and Montaña Majua have been related by Ablay *et al.* (1995) to a stratified magma chamber (albeit to different vents), our data do not support this assumption. The mineralogical and geochemical compositions of these deposits (Figs 6 and 8) are sufficiently different, thus indicating their origin from different magma chambers. In addition, Carracedo *et al.* (2007) proposed different ages for these three deposits and so they should be considered as corresponding to different eruptions.

Despite their apparent compositional homogeneity, whole-rock geochemistry and mineral chemistry allow us to distinguish different deposits and to identify them as originating from different magma batches and thus from different eruptions. This interpretation is reinforced by stress and experimental petrology studies on TPV systems, which have shown that each eruption is fed by a different batch of phonolitic magma that accumulated in a different position inside the edifice (Martí & Geyer 2009; Andújar *et al.* 2013). On the basis of major elements and mineral compositions the studied rocks can be divided roughly into two groups, a relatively more evolved group (Pico Cabras, El Boquerón, Los Gemelos, Montaña Blanca, TPV North Flank) and a less evolved group (El Calderón, Abrunco PDC and CMP, Llanos de la Santidad, Abejera, Montaña Majua). However, as was previously pointed out, the geochemical differences between the TPV phonolitic rocks are not remarkable (Ablay *et al.* 1998; Andújar *et al.* 2013). The geochemical features of the studied rocks suggest a common source for all magma batches (i.e. cogenetic in origin) and that the existing differences correspond to different evolutionary histories of the final pre-eruptive stages, which may include differences in the position of each phonolitic reservoir, in the oxygen fugacity or otherwise of pre-eruptive mixing of magmas (see Ablay *et al.* 1995; Martí *et al.* 2008; Martí & Geyer 2009; Wiesmaier *et al.* 2012; Andújar *et al.* 2013). The REE patterns indicate that the deposits at Llanos de la Santidad, El Calderón Unit I and Abrunco depart slightly from the general trend defined by the other deposits. The assessment of the mineral chemistry and geochemical features, as well as field relationships, is a useful tool for determining the stratigraphic correlations of the studied deposits.

All the pyroclastic deposits that can be correlated with a particular vent (Montaña Blanca, El Boquerón, Roques Blancos, Los Gemelos, Montaña Majua, Abrunco, Pico Cabras and Abejera) are also associated with the extrusion of lavas and/or domes of, in some cases, significant volume and extent. This indicates that in all of these cases the explosive volcanism corresponded to complex eruptions that also included effusive episodes. In some cases the explosive phase occurred at the beginning of the eruption (Montaña

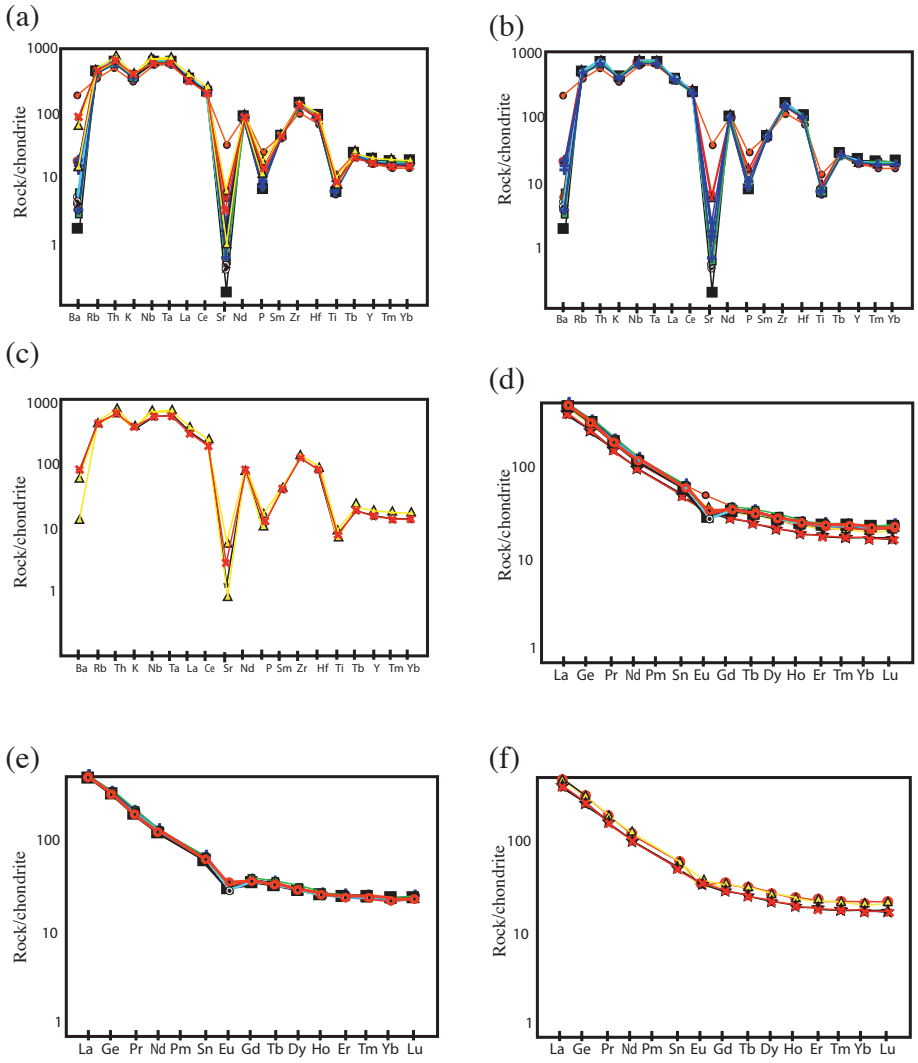

Fig. 10. (**a**–**c**) Multi-element variation diagrams normalized to chondrite values of Thompson (1982): (**a**) all pumice deposits; (**b**) Montana Blanca (black square), El Boquerón (+), Pico Cabras (arrows), Los Gemelos (grey square), TPV North Flank (double circle), Abejera (filled triangle) and Calderón Unit I (circle). (**c**) Abrunco (open star), Llanos de la Santidad (x) and Majua (light triangle). (**d**–**f**) Multi-element variation diagrams normalized to primitive mantle values of Sun & McDonough (1989): (**d**) Montana Blanca (black square), El Boquerón (+), Pico Cabras (arrow), Los Gemelos (square), TPV North Flank (double circle), Abejera (filled triangle) and Calderón Unit I (circle). (**f**) Abrunco (star), Llanos de la Santidad (x) and Majua (open triangle).

Majua, El Boquerón, Abrunco and Los Gemelos), whereas in others it took place at the end (Pico Cabras and Abejera) or even during an intermediate stage (Montaña Blanca and Roques Blancos). It is worth mentioning that none of the eruptions with identified vents occurred from the central vents; that is, there is no evidence of major explosive volcanism from the central vents. This also suggests that different eruption behaviours may have governed flank (explosive) and central eruptions (effusive). Despite using different approaches, this interpretation coincides with those of both Martí & Geyer (2009) and Andújar *et al.* (2013), who were able to demonstrate that flank eruptions are fed by reservoirs located at different depths and are subject to different stress conditions from those feeding central eruptions.

The fact that all of the studied pyroclastic deposits date from the Holocene raises the question of whether the TPV complex is entering a more explosive stage, as suggested by Martí *et al.* (2008). Although the erosion on the northern side of TPV is severe and has affected the pyroclastic deposits in this sector, it seems unlikely that older deposits, if they exist, would have been completely removed. It seems more plausible to suggest that no pyroclastic deposits were produced in previous phonolitic eruptions from TPV. Furthermore, we were unable to find any TPV pyroclastic deposits older than those identified in this study inside the calderas of Las Cañadas. Likewise, previous studies that used information from boreholes drilled inside the caldera reported no such deposits (Ablay & Martí 2000). All these findings tend to support the idea that the explosive character of TPV has increased during the Holocene. This agrees with the petrological evolution from basanites to phonolites shown by TPV magmas (Ablay *et al.* 1998; Wiesmaier *et al.* 2012) and the tendency over time to move towards more evolved phonolitic melts that are richer in volatiles (Ablay *et al.* 1998).

Conclusions

We have demonstrated the existence of at least 11 Holocene phonolitic explosive episodes, ranging from Strombolian to sub-Plinian, associated with the TPV complex, which confirm the significance of explosive volcanism in TPV during its more recent history. Field and petrological data have permitted us to establish the relative stratigraphy of these deposits and to place them within the general stratigraphy of the TPV that has been proposed in previous studies. Mineralogical and geochemical correlations, in addition to field relationships, were useful tools for determining the stratigraphic constraints of the studied deposits. We were able to recognize the sources of eight of the pyroclastic deposits, all of them fed by flank eruptions. The presence of these phonolitic pyroclastic deposits in the recent stratigraphy of the Teide–Pico Viejo complex demonstrates that phonolitic explosive activity is much more significant than previously thought and represents an important hazard for the island of Tenerife, which should be considered in hazard assessment. Moreover, the fact that all of the studied

deposits date from the Holocene and that no older deposits of similar characteristics have been identified in this study suggests that the TPV complex is entering a more explosive stage, which coincides with the evolution shown by the different phonolitic cycles identified in the pre-TPV Las Cañadas edifice.

This research was partially funded by MICINN grant CGL2008-04264, the IGN–CSIC collaboration agreement for the study of Tenerife volcanism, and the European Commission. The authors are grateful to the Teide National Park for permission to undertake this research, and to the Cabildo of Tenerife for permission FYF 412/10. We would also like to thank all the IGN staff working at the Geophysics Centre of Canarias for their support during the field campaigns, as well as the staff of the Central Geophysical Observatory, Madrid. Thanks are also due to F. Costa for his helpful comments. We thank the JGS reviewers and editor for their constructive reviews and comments.

References

Ablay, G.J. 1997. *Evolution of the Teide–Pico Viejo complex and magma system, Tenerife, Canary Islands*. PhD Thesis, University of Bristol.

Ablay, G.J. & Martí, J. 2000. Stratigraphy, structure, and volcanic evolution of the Pico Teide–Pico Viejo formation, Tenerife, Canary Islands. *Journal of Volcanology and Geothermal Research*, **103**, 175–208, doi:10.1016/s0377-0273(00)00224-9.

Ablay, G.J., Ernst, G.G.J., Martí, J. & Sparks, R.S.J. 1997. The 2 ka subplinian eruption of Montaña Blanca, Tenerife. *Bulletin of Volcanology*, **57**, 337–355.

Ablay, G.J., Carroll, M.R., Palmer, M.R., Martí, J. & Sparks, R.S.J. 1998. Basanite–phonolite lineages of the Teide–Pico Viejo volcanic complex, Tenerife, Canary Islands. *Journal of Petrology*, **39**, 905–936.

Ancochea, E., Huertas, M.J., Fuster, J.M., Cantagrel, J.M., Coello, J. & Ibarrola, E. 1999. Evolution of the Cañadas edifice and its implications for the origin of the Cañadas caldera (Tenerife, Canary Islands). *Journal of Volcanology and Geothermal Research*, **88**, 177–199.

Andújar, J., Costa, F. & Martí, J. 2010. Magma storage conditions of the last eruption of Teide volcano (Canary Islands, Spain). *Bulletin of Volcanology*, **72**, 381–395.

Andújar, J., Costa, F. & Scaillet, B. 2013. Storage conditions and eruptive dynamics of central versus flank eruptions in volcanic islands: the case of Tenerife (Canary Islands, Spain). *Journal of Volcanology and Geothermal Research*, doi:10.1016/j.jvolgeores.2013.05.004.

Araña, V. 1971 Litología y estructura del Edificio Cañadas, Tenerife. *Estudios Geológicos*, **27**, 97–135.

Araña, V., Barberi, F. & Ferrara, G. 1989. El complejo volcanico del Teide–Pico Viejo. *In*: Araña, V., Coello, J. & Araña, V. (eds) *Los volcanes y la caldera del Parque Nacional del Teide (Tenerife, Islas Canarias). Litología y Estructura del Edificio Cañadas, Tenerife (Islas Canarias)*. Estacion Geologica, **27**, 95–135.

Balcells, R. & Hernández-Pacheco, A. 1989. El domo colada de Roques Blancos. *In*: Coello, J. & Araña, V. (eds) *Los Volcanes y La Caldera del Parque Nacional del Teide (Tenerife, Islas Canarias)*. ICONA, Madrid, 227–234.

Carmichael, I.S.E. 1967. The iron–titanium oxides of salic volcanic rocks and their associated ferromagnesian silicates. *Contributions to Mineralogy and Petrology*, **14**, 36–64.

Carracedo, J.C., Paterne, M., Guillou, H., Pérez Torrado, F.J., Paris, R., Rodríguez-Bardiola, E. & Hansen, A. 2003. Dataciones radiométricas (^{14}C y K/Ar) del Teide y el rift noroeste, Tenerife, Islas Canarias. *Estudios Geológicos*, **59**, 15–29.

Carracedo, J.C., Rodríguez-Bardiola, E., *et al.* 2007. Eruptive and structural history of Teide volcano and rift zones of Tenerife, Canary Islands. *Geological Society of America Bulletin*, **119**, 1027–1051, doi:10.1130/B26087.1.

Deer, W.A., Howie, R.A. & Zussman, J. 1992. *An Introduction to the Rock-Forming Minerals*, 2nd edn. AddisonWesley Longman China, Hong Kong.

Droop, G.T.R. 1987. A general equation for estimating Fe^{3+} in ferromagnesian silicates and oxides from microprobe anaysis, using stoichiometric criteria. *Mineralogical Magazine*, **51**, 431–437.

Edgar, C.J., Wolff, J.A., *et al.* 2007. The late Quaternary Diego Hernandez Formation, Tenerife: A cycle of voluminous explosive phonolitic eruptions. *Journal of Volcanology and Geothermal Research*, **160**, 59–85.

Folch, A. & Felpeto, A. 2005. A coupled model for dispersal of tephra during sustained explosive eruptions. *Journal of Volcanology and Geothermal Research*, **145**, 337–349, doi:10.1016/j.jvolgeores.2005.01.010.

García, O., Martí, J., Aguirre-Díaz, G., Geyer, A. & Iribarren, I. 2011. Pyroclastic density currents from Teide–Pico Viejo (Tenerife, Canary Islands): Implications on hazard assessment. *Terra Nova*, **23**, 220–224, doi:10.1111/j.1365-3121.2011.01002.x.

García, O., Bonadonna, C., Martí, J. & Pioli, L. 2012. The 5,660 y BP Boquerón explosive eruption, Teide–Pico Viejo complex, Tenerife. *Bulletin of Volcanology*, **74**, 2037–2050, doi:10.1007/s00445-012-0646-5.

Hausen, H. 1956. Contributions to the geology of Tenerife. *Societas Scientiarum Fennica, Commentationes Physico-Mathematicae*, **18**, 1–247.

Le Bas, M.J., Le Maitre, R.W., Streckeisen, A. & Zanettin, B. 1986. A chemical classification of volcanic rocks based on the total alkali–silica diagram. *Journal of Petrology*, **27**, 745–754.

Martí, J. & Geyer, A. 2009. Central vs flank eruptions at Teide–Pico Viejo twin stratovolcanoes (Tenerife, Canary Islands). *Journal of Volcanology and Geothermal Research*, **181**, 47–60.

Martí, J. & Gudmundsson, A. 2000. The Las Cañadas caldera (Tenerife, Canary Islands): an overlapping collapse caldera generated by magma-chamber migration. *Journal of Volcanology and Geothermal Research*, **103**, 161–173.

Martí, J.A., Mitjavila, J. & Araña, V. 1994. Stratigraphy, structure and geochronology of the Las Cañadas caldera (Tenerife, Canary Islands). *Geological Magazine*, **131**, 715–717.

Martí, J., Hurlimann, M., Ablay, G.J. & Gudmundsson, A. 1997. Vertical and lateral collapses in Tenerife and other ocean volcanic islands. *Geology*, **25**, 879–882.

Martí, J., Geyer, A., Andujar, J., Teixó, F. & Costa, F. 2008. Assessing the potential for future explosive activity from Teide–Pico Viejo stratovolcanoes (Tenerife, Canary Islands). *Journal of Volcanology and Geothermal Research*, **178**, 529–542, doi:10.1016/j.jvolgeores.2008.07.011.

Martí, J., Sobradelo, R., Felpeto, A. & García, O. 2011. Eruptive scenarios of phonolitic volcanism at Teide–Pico Viejo volcanic complex (Tenerife, Canary Islands). *Bulletin of Volcanology*, **74**, 767–782, doi:10.1007/s00445-011-0569-6.

Morimoto, N. 1988 Nomenclature of pyroxenes. *American Mineralogist*, **73**, 1123–1133.

Pérez Torrado, F.J., Carracedo, J.C., Paris, R. & Hansen, A. 2004. Descubrimientos de depósitos freatomagmáticos en las calderas septentrionales de estratovolcan Teide (Tenerife, Islas Canarias): relaciones estratigraficas e implicaciones volcánicas. *Geotemas*, **6**, 163–166.

Reimer, P.J., Baillie, M.G.L., *et al.* 2004. INTCAL04 terrestrial radiocarbon age calibration, 0-26 cal kyr BP. *Radiocarbon*, **46**, 1029–1058.

Ridley, W. 1970. The abundance of rock types on Tenerife, Canary Islands, and its petrogenetic significance. *Bulletin of Volcanology*, **34**, 196–204.

Szramek, L., Gardner, J. & Larsen, J. 2006. Degassing and microlite crystallization of basaltic andesite magma erupting at Arenal Volcano, Costa Rica. *Journal of Volcanology and Geothermal Research*, **157**, 182–201, doi:10.1016/j.volgeores.2006.03.039.

Sun, S. & McDonough, W.F. 1989. Chemical and isotopic systematics of oceanic basalts: implications for mantle composition and processes. *In*: Saunders, A.D. & Norry, M.J. (eds) *Magmatism in the Ocean Basins*. Geological Society, London, Special Publications, **42**, 313–345, doi:10.1144/GSL.SP.1989.042.01.19.

Thompson, R.N. 1982. Magmatism of the British Tertiary province. *Scottish Journal of Geology*, **18**, 49–107.

Tischendorf, G., Gottesmann, B., Föster, H.J. & Trumbull, R.B. 1997. On Li-bearing micas: estimating Li from electron microprobe analyses and improved diagram for graphical representation. *Mineralogical Magazine*, **61**, 809–834.

Triebold, S., Kronz, A. & Gerhard, W. 2006. Anorthite-calibrated backscattered electron profiles, trace elements and growth textures in feldspars from Teide–Pico Viejo volcanic complex (Tenerife). *Journal of Volcanology and Geothermal Research*, **154**, 117–130, doi:10.1016/j.jvolgeores.2005.09.023.

Wiesmaier, S., Deegan, F.M., Troll, V.R., Carracedo, J.C., Chadwick, J.P. & Chew, D.M. 2011. Magma mixing in the 1100 AD Montaña Reventada composite lava flow, Tenerife, Canary Islands: interaction between rift zone and central volcano plumbing systems. *Contributions to Mineralogy and Petrology*, **162**, 651–669.

Wiesmaier, S., Troll, V.R., Carracedo, J.C., Ellam, R.M., Bindeman, I. & Wolf, J. 2012. Bimodality of lavas in the Teide–Pico Viejo succession in Tenerife, the role of crustal melting in the origin of recent phonolites. *Journal of Petrology*, **53**, 2465–2495.

Wright, H.M.N., Cashman, K.V., Rosi, M. & Cioni, R. 2006. Breadcrust bombs as indicators of vulcanian eruptions at Guagua Pichincha volcano, Ecuador. *Bulletin of Volcanology*, **69**, 281–300, doi:10.1007/s00445-006-0073-6.

Yavurt, F. 2001. LIMICA: a program for estimating Li from electron-microprobe mica analyses and classifying trioctahedral micas in terms of composition and octahedral site occupancy. *Computers and Geosciencies*. **27**, 215–227.

Received 19 July 2013; revised typescript accepted 12 January 2014.
Scientific editing by David Pyle.

GEOFACETS from ELSEVIER + The Geological Society *serving science & profession*

The Geofacets-GSL Millennium Edition

Geofacets from Elsevier is an innovative web-based research tool designed by geoscientists for geoscientists. Elsevier and the Geological Society of London (GSL) have partnered together to provide GSL members with a unique opportunity to gain individual access to thousands of geological maps from the renowned Lyell Collection through the Geofacets platform.

USE SEARCH FEATURES DESIGNED FOR GEOSCIENTISTS:

- Search for map content via an interactive map interface
- Refine results by map type, surface area and geological basin
- Search for specific terms, geological deposit models or analogs

EXCLUSIVE TO MEMBERS OF THE GEOLOGICAL SOCIETY OF LONDON

ONLY £35/YR

Lyell Collection
Geological Society publications online

DISCOVER AND DOWNLOAD MAPS:

- 24,000+ downloadable maps from the Lyell Collection
- 16,000+ available as GeoTIFFS for easy integration
- Each map is accompanied by metadata
- Includes source information and full-text PDF
- Continuously updated with newly published maps

SUPERCHARGE YOUR GSL MEMBERSHIP WITH THE GEOFACETS-GSL MILLENNIUM EDITION.

Email membership@geolsoc.org.uk to sign up today!

TOTAL NUMBER OF MAPS: **24,000+**
With 16,000+ georeferenced

MAP SUBJECT AREA COVERAGE*

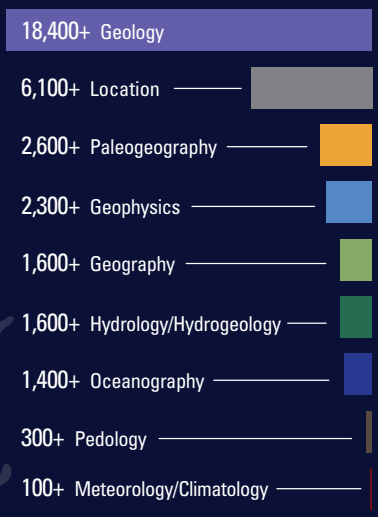

*Categorization of maps by subject area is not mutually exclusive. Maps may fall under multiple categories.